Synthesis and corrosion behavior of a hybrid bioceramic–biopolymer coating on biodegradable Mg alloy for orthopaedic implants

Article *in* Journal of Alloys and Compounds · July 2015

Impact Factor: 3 · DOI: 10.1016/j.jallcom.2015.07.075

8 authors, including:

Hamid Reza Bakhsheshi-Rad
Universiti Teknologi Malaysia
71 PUBLICATIONS **430** CITATIONS
SEE PROFILE

Esah Hamzah
Universiti Teknologi Malaysia
150 PUBLICATIONS **462** CITATIONS
SEE PROFILE

Ahmad Fauzi Ismail
Universiti Teknologi Malaysia
645 PUBLICATIONS **9,271** CITATIONS
SEE PROFILE

Safaa Saud
Management and Science University
33 PUBLICATIONS **65** CITATIONS
SEE PROFILE

Journal of Alloys and Compounds 648 (2015) 1067–1071

Contents lists available at ScienceDirect

Journal of Alloys and Compounds

journal homepage: http://www.elsevier.com/locate/jalcom

Letter

Synthesis and corrosion behavior of a hybrid bioceramic-biopolymer coating on biodegradable Mg alloy for orthopaedic implants

Keywords:
Magnesium
Polycaprolactone
Octacalcium phosphate
Biodegradable
Corrosion

A B S T R A C T

A composite coating composed of octacalcium phosphate (OCP) and hydroxyapatite (HA) as an underlayer and polycaprolactone (PCL) as an overlayer was fabricated on an Mg–1.2Ca–2Zn alloy *via* combination of chemical solution deposition and dip coating methods. The overlayer was composed of a pore network structure with thickness around 38 μm but the underlayer consisted of plate-like crystals with inner dense layer (1.2 μm) and an outer coarse layer (6 μm). The corrosion current densities of Mg alloy significantly decreased after composite coating from 211.6 to 0.059 μA/cm^2. Hence, the PCL/OCP/HA composite coating can effectively protect the Mg–1.2Ca–2Zn alloy when used as degradable orthopaedic implants.

1. Introduction

Magnesium alloys as biodegradable/bioabsorbable materials have great potential for orthopaedic and cardiovascular applications [1]. However, the rapid degradation rate of magnesium under physiological conditions prevents human tissue from healing completely [2]. Numerous investigations into controlling the rapid corrosion rate of Mg alloys have been carried out including surface modification [3,4]. Polymeric coating on magnesium surfaces is a well-known and interesting approach to enhance corrosion resistance of the alloy because the polymer layer can act as a barrier, preventing the reaction between the metal and corrosive ions [5]. PCL (–[$(CH_2)_5COO$]–) is a promising polymer due to its high toughness and biocompatibility as well as remarkable mechanical properties, such as 80% elongation at break point [6,7]. PCL coating can enhance the in-vitro corrosion behavior and protect the implant from rapid degradation [6,7]. However, the application of PCL coating for bone regeneration is limited because of low stiffness, hydrophobic nature, and relatively low bioactivity [8]. To address this problem, calcium phosphate coating, such as HA ($Ca_{10}(PO_4)_6(OH)_2$) and OCP ($Ca_8H_2(PO_4)_6.5H_2O$) is used to control the corrosion rate and enhance bone conductivity of the alloy [9]. HA is the main mineral phase in natural bone which can enhance biological therapies as well as showing good bioactivity and osteoconductivity as a coating material [1,10]. OCP is a salt which is a proposed precursor of bone and tooth apatite crystals and is involved in initial intramembranous bone formation [10]. Furthermore, synthetic OCP as a source material for bone substitutes can be essential for the regeneration of bones and is suitable for treating various kinds of bone defects [10,11]. In this study, HA and OCP coatings as underlayer was prepared by single-step chemical solution. PCL was prepared as an overlayer fabricated by dip coating on an Mg alloy. The relationship between the microstructure and corrosion behavior of the composite coated magnesium alloy was also evaluated.

2. Experimental synthesis

Mg–1.2Ca–2Zn alloy samples with dimensions of 15 mm × 10 mm × 10 mm were used as substrates. The chemical solution deposition was applied for coating of OCP/HA on Mg alloy according to Tomozawa et al. [9]. The solution was prepared with 0.25 mol/L Ca-EDTA ($C_{10}H_{12}N_2O_8Na_2Ca$) and 0.25 mol/L KH_2PO_4. The pH value of the solution was adjusted to 5.0 by adding HNO_3 and $(CH_2OH)_3CNH_2$ at room temperature. The Mg alloy samples were immersed into the solution and kept at 90 °C for 2 h. Prior to dipping the OCP/HA coated sample, 2.5 wt.% PCL pellets (Mw = 80,000 g/mol, Sigma–Aldrich, UK) were dissolved in dichloromethane (DCM; CH_2Cl_2, Sigma–Aldrich, UK) by stirring for 6 h at room temperature. The coated samples were dipped for 30 s and withdrawn at a constant speed to form a uniform coating and then dried at room temperature. X-ray diffractometry (Siemens-D500) was used to identify the phases present in the specimens using Cu Kα radiation generated at 40 kV and 35 mA. The crystallite size was determined by the Scherrer equation [12]. Fourier-transformed infrared (FTIR) spectroscopy was used to determine the surface functional groups of the coating samples. The FTIR spectrum was recorded in a spectral range of 4000–400 cm^{-1}. Microstructural observation was performed using a scanning electron microscope (SEM; JEOL JSM-6380LA) and transmission electron microscopy (HT7700 Hitachi).

Rectangular specimens with a surface area of 1 cm^2 were embedded in epoxy resin for electrochemical testing. Corrosion testing was conducted at 37 °C in an open air glass cell containing

http://dx.doi.org/10.1016/j.jallcom.2015.07.075
0925-8388/

350 mL static solution of simulated body fluid (SBF) (Kokubo) with an initial pH of 7.4 using a potentiostat (PARSTAT 2263 Princeton Applied Research). A three-electrode cell was used for potentiodynamic polarization (PDP) tests where a saturated calomel electrode (SCE) was used as the reference electrode, a graphite rod as the counter electrode, and an alloy specimen as the working electrode. The samples were immersed in the SBF for 1 h prior to the PDP test to establish the open-circuit potential for providing uniform corrosion and well-defined Tafel region [13]. PDP experiments (n = 3) were carried out at a constant scan rate of 0.166 mV/s, and initiated at −250 mV below the open-circuit potential. The electrochemical impedance spectra (EIS) were measured at 10 mV sine amplitude over a frequency range of 1 Hz–100 kHz using a VersaSTAT 3 machine. Each electrochemical test was repeated 3 times to confirm reproducibility of the results. EIS results were fitted to a suitable model circuit using ZSimWin software.

3. Results and discussion

3.1. Microstructure characterization

Fig. 1a–c shows that the ternary Mg–1.2Ca–2Zn alloy consists of α–Mg, Mg_2Ca and $Ca_2Mg_6Zn_3$ which is consistent with the Mg–Ca–Zn phase diagram [12,14]. The presence of secondary phase can significantly affect the corrosion behavior of the Mg alloy due to the formation of micro-galvanic cells between the matrix and secondary phases [15]. The EDS analysis showed that tri-pole junction of the grain boundaries were enriched with zinc and calcium which indicates the formation of Mg_2Ca and $Ca_2Mg_6Zn_3$ (Fig. 1d). The OCP/HA coating formed on the surface of the magnesium alloy was composed of plate-like crystals which formed an open network. OCP/HA coating consisted of pores having several tens of nanometer in size (Fig. 1e–g) that presumably reduces the corrosion resistance if used without top coating. This is consistent with the findings of Tomozawa et al. [9]. EDS analysis clearly showed that the coating consisted of Ca, P and O while the Mg and Zn peaks (Fig. 1h) are from the substrate. The atomic ratio of Ca/P in the coatings was about 1.37 which is between the Ca/P ratios of OCP and HA. The PCL/OCP/HA coating consisted of interconnected pore networks which were free of visible defects on the surface and uniformly distributed on the Mg substrate. In this regard, PCL homogenously cover the OCP/HA layer (Fig. 1i–k) which serves as a barrier against corrosive electrolytes. This is expected to improve the corrosion resistance of the coated sample. EDS analysis also resulted in the detection of C, O, and Mg in this sample, indicating the formation of PCL as can be seen in Fig. 1l.

Fig. 2a shows a cross-sectional SEM image of the OCP/HA coated Mg alloy specimen, indicating porous coating with relatively uniform thickness (6–8 μm). High magnification images show the longitudinal growth of plate-like crystals of OCP, which grew along their (001) direction. Furthermore, it can be observed that the coating consists of HA as an inner dense layer and OCP as an outer coarse layer which are in agreement with the results of Tomozawa et al. [9]. The inner layer clearly has pores that are nanometers in size. However, the PCL/OCP/HA coating indicated two distinct layer structures, the PCL layer (35–40 μm) at the top and OCP/HA with a thickness of around 6–8 μm underneath (Fig. 2b). The porous structure of PCL with diameters of less than 10 μm can be clearly seen in the micrographs. In this regards, thickness, density/porosity and uniformity of the coating have considerable roles in protecting against corrosion [9,16]. Degner et al. [17] showed that PCL coating can effectively prevent magnesium alloys from corrosion which related to the polymer film thickness. Thus, the PCL/OCP/HA coating is expected to exhibit a higher degree of protection.

TEM image and corresponding selected area diffraction patterns (SADP) of the OCP coating show the crystal was a long flattened plate with width and thickness of about 800 and 45 nm respectively (Fig. 2c), where the surfaces and the edges of the crystals are flat and smooth. The diffraction pattern was identified as (1 0 0). The diffraction pattern of the other plate-like crystals also corresponded to OCP and the plates grew parallel to the (1 0 0). After

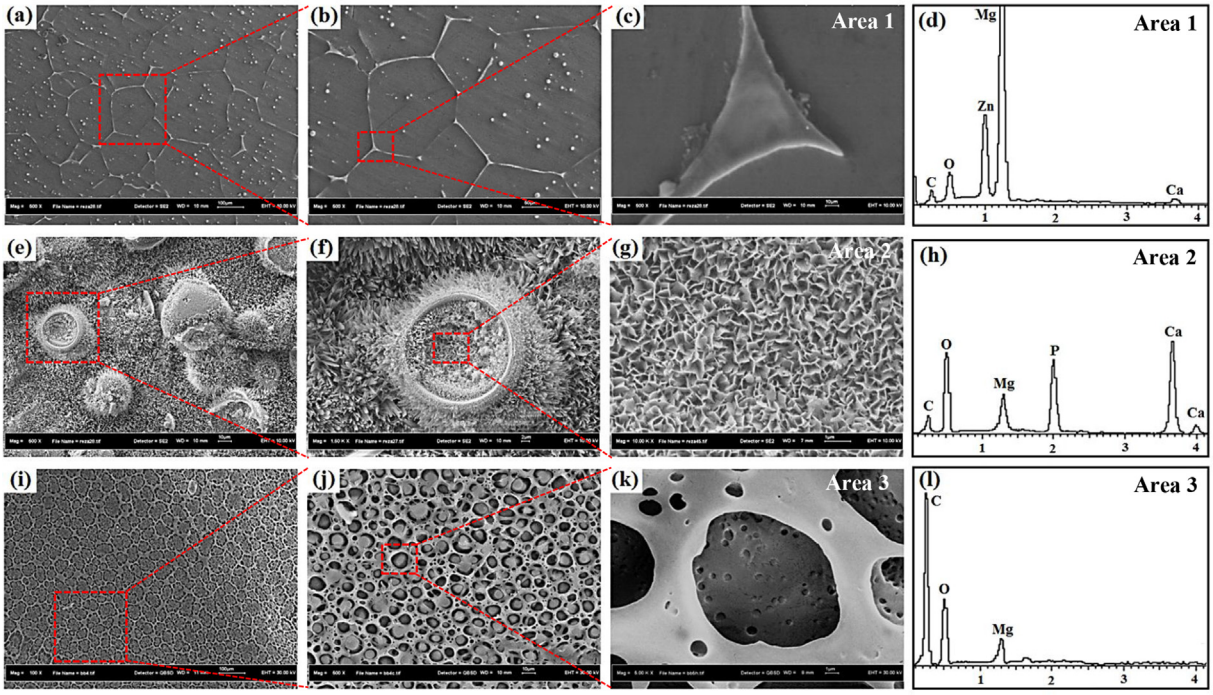

Fig. 1. Scanning electron micrographs of the surface of (a,b,c) uncoated Mg–Ca–Zn, (e,f,g) OCP/HA coated Mg–Ca–Zn, and (i,j,k) PCL/OCP/HA coated Mg–Ca–Zn; and EDS analysis of (d) Area 1 (h) Area 2 and (l) Area 3.

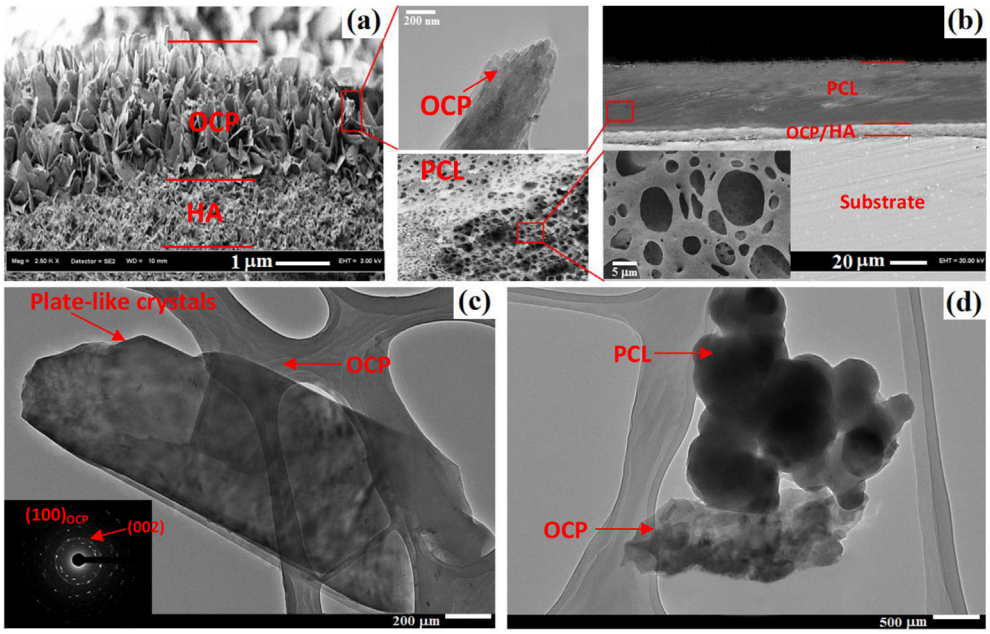

Fig. 2. Scanning electron micrographs of the cross-section of (a) OCP/HA-coated and (b) PCL/OCP/HA coated Mg–Ca–Zn. Insets show higher magnification images. Transmission electron micrograph of (c) OCP/HA coated and (d) PCL/OCP/HA coated Mg–Ca–Zn sample.

coating with a PCL layer as the top layer, dark spherical particles can be observed that are assumed to be PCL (Fig. 2d).

The XRD results of the ternary Mg–1.2Ca–2Zn alloy (Fig. 3a) show that the alloy consists of Mg, Mg_2Ca and $Ca_2Mg_6Zn_3$ which is consistent with the SEM/EDS results. However, the XRD patterns of the underlayer shows the characteristic peaks of the OCP/HA ($2\theta = 4.9°$, 26° and 48°), corresponding to (0 1 0), (2 0 0) and (0 0 4) planes, respectively [1]. The peak at 4.7° is related to OCP (PDF No. 44-0778) while two other peaks (26° and 48°) could be attributed to both OCP and HA (PDF No. 09-0432) due to overlapping. The calculated crystallite size in the OCP/HA coating sample is 64 nm. The PCL/OCP/HA background spectrum mainly consists of two intense peaks for PCL ($2\theta = 21.6°$ and 23.8°) [18], which related to diffraction on the (1 1 0) and (2 0 0) planes respectively (PCL has a crystalline structure with polyethylene-like orthorhombic cell disposition, with lattice parameters a = 0.748 nm, b = 0.498 nm and c = 1.727 nm) [18].

The FTIR spectra of OCP/HA (Fig. 3b) shows characteristic peaks of sharp P–O bands at 1113 and 1046 cm^{-1}, which are typical of the OCP structure [1]. The HPO_4^{2-} band at 908 and 872 cm^{-1} was attributed to the librational mode (ν_L) of the hydroxyl group, which further confirmed the crystalline nature of HA. Two PO_4^{3-} sharp bands at 560–600 cm^{-1} correspond to OCP indicating a well-developed crystalline structure [19]. The C–O stretching band at 1460 and 1420 cm^{-1} indicate the partial substitution of the PO_4^{3-} group of OCP and HA with CO_3^{2-}. O–H bands were found at 1642 cm^{-1}. However, the FTIR spectrum of the PCL/OCP/HA composite sample include: (1) $-(CH_2)-$ skeletal group in the range of 2978–2812 cm^{-1} and 1465–1226 cm^{-1}; (2) C=O band centred at 1612 cm^{-1}; and (3) C–O groups in the range 1253–1114 cm^{-1}. The strong absorption of the C=O bond was indicative of an aliphatic ester of PCL on the surface [20]. The FTIR spectrum further confirmed the formation of a OCP/HA and PCL/OCP/HA layered film.

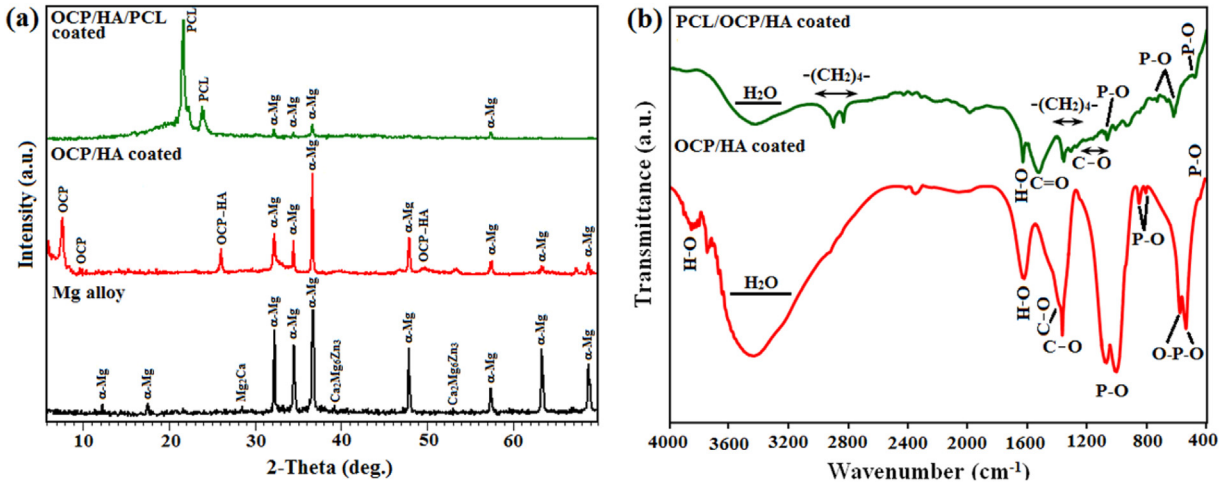

Fig. 3. (a) X-ray diffraction patterns and (b) Fourier-transformed infrared for the uncoated, OCP/HA coated and PCL/OCP/HA coated Mg–Ca–Zn sample.

3.2. Corrosion behavior

Fig. 4a shows the cathodic and anodic polarization curves of the uncoated and coated specimens in the Kokubo solution. The corrosion potentials (E_{corr}) of the uncoated Mg–1.2Ca–2Zn, OCP/HA and PCL/OCP/HA-coated specimens were −1631.2 mV_{SCE}, −1529.4 mV_{SCE} and −1259.1 mV_{SCE}, respectively. The reason for the more negative corrosion potential of the uncoated Mg–1.2Ca–2Zn when compared to the coated alloy is due to the formation of a microgalvanic cell between α-Mg and the secondary phases. However, the PCL/OCP/HA-coated specimen presented more positive E_{corr} than OCP/HA coated and uncoated. This can be attributed to the formation of a PCL film as the top layer and OCP/HA as an inner layer preventing infiltration of aggressive solution into the coating during corrosion [12,21]. The corrosion current densities (i_{corr}) of the uncoated, OCP/HA and PCL/OCP/HA-coated specimens were 211.6, 6.15 and 0.059 μA/cm^2, respectively. Both coated samples exhibited a significantly lower i_{corr} than the uncoated sample indicating lower corrosion rates of coated samples. The Nyquist curves of the uncoated and coated samples in Fig. 4b showed a single capacitive loop at all high frequencies, while the loops of OCP/HA and PCL/OCP/HA coating have significantly larger diameters compared with the uncoated sample. The high frequency capacitive semicircle has been attributed to the charge transfer resistance, which is much larger in OCP/HA/PCL coated Mg sample than that of OCP/HA coated sample. The weak response of the high frequency capacitive semicircles indicated that the OCP/HA coating could not provide a high level of corrosion protection for the substrate due to the presence of a large number of nano-pores on the surface of the OCP/HA coating. So, this ceramic layer should be sealed by a compact hydrophobic polymer coating. The presence of PCL coating as a top layer sealed the porosity of OCP/HA coating and interrupted penetration of solution containing Cl^- ions into coating/substrate interface thus enhancing the protective performance of the coating of Mg alloy. The equivalent circuit depicted in Fig. 4c was used to fit the impedance spectra in Fig. 4b whereby R_e represents the solution resistance, C_c is the coating capacitance, C_{dl} is the double layer capacitance and R_{ct} is the charge transfer resistance which is attributed to the electrochemical corrosion rate. The equivalent circuit in Model A is employed to characterize an uncoated sample while Model B could describe the coated samples. It can be seen that the charge transfer resistance (R_{ct}) of the PCL/OCP/HA coating (2347.2 kΩ cm^2) and OCP/HA coating (8.37 kΩ cm^2) is significantly higher than that of uncoated sample (2.52 kΩ cm^2). This is attributed to the fact that the PCL coating on the top of OCP/HA layer could seal the nano-pores and provide better protection for the Mg substrate [22]. The Bode plot (Fig. 4d) demonstrated that OCP/HA/PCL has the highest impedance as compared to lower impedance at 1 Hz for OCP/HA coated sample which was attributed to the poor barrier characteristic of the coating. The PCL as a top layer on OCP/HA modified the porous structure of the OCP/HA layer by the formation of a thick, densely packed and crack-free coating, which noticeably decreased the corrosion rate of the Mg alloy substrate. At the same time OCP/HA as an underlayer with dense inner layer can further prevent the penetration of aggressive solutions to the Mg alloy.

4. Conclusion

A novel combination of chemical solution deposition and dip coating methods were conducted to fabricate composite coating on the Mg–1.2Ca–2Zn alloy. The composite coating consisted of

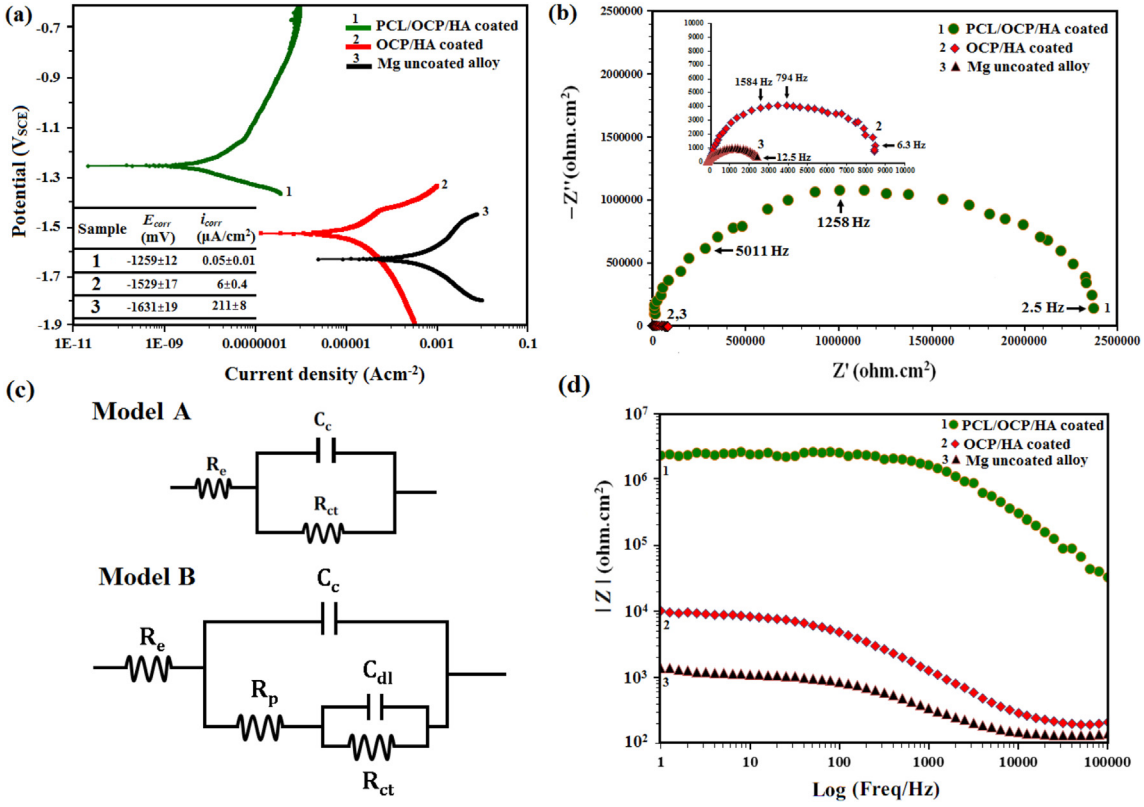

Fig. 4. (a) Potentiodynamic polarization curves, (b) Nyquist plot, (c) Equivalent electrical circuit for uncoated (Model A) and coated samples (Model B), (d) Bode plot for the uncoated, OCP/HA coated and PCL/OCP/HA coated Mg–Ca–Zn sample in Kokubo solution.

overlayer of PCL (35–40 μm) and underlayer of OCP/HA (6–8 μm). The PCL layer consisted of pore networks which were free of defects on the surface but, OCP/HA layer composed of dense inner layer and coarse outer layer with plate-like crystals. OCP/HA as an underlayer affects the microstructure of the PCL coated layer and hence improves the corrosion resistance of the Mg alloy. The results showed that the PCL/OCP/HA composite coating can provide high level of protection and decrease significantly corrosion rate of the Mg–1.2Ca–2Zn alloy.

Acknowledgments

The author(s) would like to thank the Malaysian Ministry of Higher Education (MOHE) and Universiti Teknologi Malaysia for providing the financial support and facilities for this research.

References

[1] S. Hiromoto, M. Inoue, T. Taguchi, M. Yamane, N. Ohtsu, Acta Biomater. 11 (2015) 520–530.
[2] Y. Xiong, C. Lu, C. Wang, R. Song, J. Alloys Compd. 625 (2015) 258–265.
[3] M. Daroonparvar, M.A.M. Yajid, N.M. Yusof, H.R. Bakhsheshi-Rad, J. Alloys Compd. 645 (2015) 450–466.
[4] M. Daroonparvar, M.A.M. Yajid, N.M. Yusof, H.R. Bakhsheshi-Rad, E. Hamzah, H.A. Kamali, J. Alloys Compd. 615 (2014) 657–671.
[5] T.F. da Conceicao, N. Scharnagl, W. Dietzel, K.U. Kainer, Corros. Sci. 53 (2011) 338–346.
[6] H.M. Wong, K.W.K. Yeung, K.O. Lam, V. Tam, P.K. Chu, K.D.K. Luk, K.M.C. Cheung, Biomaterials 31 (2010) 2084–2096.
[7] S.I. Roohani-Esfahani, S. Nouri-Khorasani, Z. Lu, R. Appleyard, H. Zreiqat, Biomaterials 31 (2010) 5498–5509.
[8] E.J. Lee, S.H. Teng, T.S. Jang, P. Wang, S.W. Yook, H.E. Kim, Y.H. Koh, Acta Biomater. 6 (2010) 3557–3565.
[9] M. Tomozawa, S. Hiromoto, Acta Mater. 59 (2011) 355–363.
[10] O. Suzuki, Acta Biomater. 6 (2010) 3379–3387.
[11] O. Suzuki, Jpn. Dent. Sci. Rev. 49 (2013) 58–71.
[12] H.R. Bakhsheshi-Rad, E. Hamzah, M. Daroonparvar, S.N. Saud, M.R. Abdul-Kadir, Vacuum 110 (2014) 127–135.
[13] E. McCafferty, Corros. Sci. 47 (2005) 3202–3215.
[14] M. Mezbahul-Islam, Y.N. Zhang, C. Shekhar, M. Medraj, Calphad 46 (2014) 134–147.
[15] H.Y. Tok, E. Hamzah, H.R. Bakhsheshi-Rad, J. Alloys Compd. 640 (2015) 335–346.
[16] X.N. Gu, W. Zheng, Y. Cheng, Y.F. Zheng, Acta Biomater. 5 (2009) 2790–2799.
[17] J. Degner, F. Singer, L. Cordero, A.R. Boccaccini, S. Virtanen, Appl. Surf. Sci. 282 (2013) 264–270.
[18] M. Lebourg, J. Suay Antón, J.L.G. Ribelles, Compos. Sci. Technol. 70 (2010) 1796–1804.
[19] T. Handa, T. Anada, Y. Honda, H. Yamazaki, K. Kobayashi, N. Kanda, S. Kamakura, S. Echigo, O. Suzuki, Acta Biomater. 8 (2012) 1190–1200.
[20] D.W. Hong, Z.T. Lai, T.S. Fu, T.T. Tsai, I.M. Chu, P.L. Lai, Compos. Sci. Technol. 83 (2013) 64–71.
[21] M. Ren, S. Cai, T. Liu, K. Huang, X. Wang, et al., J. Alloys Compd. 591 (2014) 34–40.
[22] H.R. Bakhsheshi-Rad, E. Hamzah, M.R. Abdul-Kadir, M. Daroonparvar, M. Medraj, Vacuum 119 (2015) 95–98.

H.R. Bakhsheshi-Rad*
Department of Materials, Manufacturing and Industrial Engineering, Faculty of Mechanical Engineering, Universiti Teknologi Malaysia, 81310 Johor Bahru, Johor, Malaysia

E. Hamzah
Department of Materials, Manufacturing and Industrial Engineering, Faculty of Mechanical Engineering, Universiti Teknologi Malaysia, 81310 Johor Bahru, Johor, Malaysia

A.F. Ismail
Advanced Membrane Technology Research Center (AMTEC), Universiti Teknologi Malaysia, 81310 Skudai, Johor Bahru, Johor, Malaysia

Z. Sharer
UTM-MPRC, Institute for Oil and Gas, Universiti Teknologi Malaysia, 81310 Skudai, Johor, Malaysia

M.R. Abdul-Kadir
Department of Materials, Manufacturing and Industrial Engineering, Faculty of Mechanical Engineering, Universiti Teknologi Malaysia, 81310 Johor Bahru, Johor, Malaysia

M. Daroonparvar
Department of Materials, Manufacturing and Industrial Engineering, Faculty of Mechanical Engineering, Universiti Teknologi Malaysia, 81310 Johor Bahru, Johor, Malaysia

Safaa N. Saud
Department of Materials, Manufacturing and Industrial Engineering, Faculty of Mechanical Engineering, Universiti Teknologi Malaysia, 81310 Johor Bahru, Johor, Malaysia

M. Medraj
Department of Mechanical Engineering, Concordia University, 1455 De Maisonneuve Blvd., West Montreal, QC H3G 1M8, Canada

Mechanical and Materials Engineering Department, Masdar Institute, PO Box 54224, Abu Dhabi, United Arab Emirates

* Corresponding author.
E-mail addresses: rezabakhsheshi@gmail.com, bhamidreza2@live.utm.my (H.R. Bakhsheshi-Rad).

14 May 2015
Available online 15 July 2015